

AD \_\_\_\_\_

Award Number: W81XWH-04-1-0360

TITLE: RhoGTPase involvement in breast cancer migration and invasion

PRINCIPAL INVESTIGATOR: Kaylene J. Simpson, Ph.D.

CONTRACTING ORGANIZATION: Harvard Medical School  
Boston, MA 02115-5701

REPORT DATE: March 2008

TYPE OF REPORT: Annual Summary

PREPARED FOR: U.S. Army Medical Research and Materiel Command  
Fort Detrick, Maryland 21702-5012

DISTRIBUTION STATEMENT: Approved for Public Release;  
Distribution Unlimited

The views, opinions and/or findings contained in this report are those of the author(s) and should not be construed as an official Department of the Army position, policy or decision unless so designated by other documentation.

REPORT DOCUMENTATION PAGE				Form Approved OMB No. 0704-0188	
Public reporting burden for this collection of information is estimated to average 1 hour per response, including the time for reviewing instructions, searching existing data sources, gathering and maintaining the data needed, and completing and reviewing this collection of information. Send comments regarding this burden estimate or any other aspect of this collection of information, including suggestions for reducing this burden to Department of Defense, Washington Headquarters Services, Directorate for Information Operations and Reports (0704-0188), 1215 Jefferson Davis Highway, Suite 1204, Arlington, VA 22202-4302. Respondents should be aware that notwithstanding any other provision of law, no person shall be subject to any penalty for failing to comply with a collection of information if it does not display a currently valid OMB control number. <b>PLEASE DO NOT RETURN YOUR FORM TO THE ABOVE ADDRESS.</b>					
1. REPORT DATE 28-03-2008		2. REPORT TYPE Annual Summary		3. DATES COVERED 1 MAR 2004 - 28 FEB 2008	
4. TITLE AND SUBTITLE RhoGTPase involvement in breast cancer migration and invasion				5a. CONTRACT NUMBER	
				5b. GRANT NUMBER W81XWH-04-1-0360	
				5c. PROGRAM ELEMENT NUMBER	
6. AUTHOR(S) Kaylene J. Simpson, Ph.D.  Email: kaylene_simpson@hms.harvard.edu				5d. PROJECT NUMBER	
				5e. TASK NUMBER	
				5f. WORK UNIT NUMBER	
7. PERFORMING ORGANIZATION NAME(S) AND ADDRESS(ES)  Harvard Medical School Boston MA 02115-5701				8. PERFORMING ORGANIZATION REPORT NUMBER	
9. SPONSORING / MONITORING AGENCY NAME(S) AND ADDRESS(ES) U.S. Army Medical Research and Materiel Command Fort Detrick, Maryland 21702-5012				10. SPONSOR/MONITOR'S ACRONYM(S)	
				11. SPONSOR/MONITOR'S REPORT NUMBER(S)	
12. DISTRIBUTION / AVAILABILITY STATEMENT Approved for Public Release; Distribution Unlimited					
13. SUPPLEMENTARY NOTES					
14. ABSTRACT  Using a high throughput small interfering RNA approach (siRNA) I screened 1081 human genes (kinases, phosphatases and a library of migration and adhesion related genes) using an automated wound healing assay to identify genes that regulate cell migration using the normal mammary epithelial cell line MCF10A. After extensive validation using other siRNAs and shRNAs I identified 66 High Confidence (HC) genes that Accelerate or Inhibit cell motility. Of these genes, 42 have no prior association with cell motility or adhesion and of these, 12 are uncharacterized with respect to any biological process. The migration pattern for the 66 HC genes were established using time-lapse video microscopy and revealed that a significant proportion of the genes that accelerate migration do so by disruption of cell-cell adhesion and adoption of highly erratic and random cell motility. These represent novel targets for future studies relating to breast carcinoma progression.					
15. SUBJECT TERMS  Breast cancer, metastasis, tumour biology, Rho GTPases, cell signalling, integrins, siRNA screening, wound healing					
16. SECURITY CLASSIFICATION OF:			17. LIMITATION OF ABSTRACT	18. NUMBER OF PAGES	19a. NAME OF RESPONSIBLE PERSON
a. REPORT	b. ABSTRACT	c. THIS PAGE			USAMRMC
U	U	U	UU	31	19b. TELEPHONE NUMBER (include area code)

## Table of contents

	Page
Introduction.....	4
Body.....	4
Key Research Accomplishments.....	7
Reportable Outcomes.....	7
Conclusion .....	8
References.....	8
Appendices.....	9

## Introduction

This project has focused on gene discovery with the broad Aim of identifying novel regulators of cell motility using an siRNA screening approach. Modulating gene expression in a normal mammary epithelial cell background has enabled us to identify genes that have positive or negative effects on cell adhesion and migration and identify candidate genes and pathways that may be critical for regulating breast tumourigenesis. The fourth year of this project (a no-cost extension) enabled extensive validation of the screening data, yielding a High Confidence dataset that was then analysed by time-lapse video microscopy to evaluate cell-cell adhesion, morphology and the speed and directionality of cells after wounding. From these studies we now have a sub-group of genes that will be refined further by analysis in a panel of *in vitro* assays and multiple cell lines, leading to our goal of analysing several targets *in vivo* and in primary breast tissue arrays.

## Body – progress report

***AIM 4: Develop high throughput siRNA screening technology to take an unbiased approach to identify novel genes that regulate motility and invasion of breast cells.***

*Aim 4.1 – complete screening of the migration-related siRNA library initiated in the pilot study phase.*

*Aim 4.2 – screen the human protein kinase and phosphatase siRNA libraries using the wound healing approach.*

Both Aims were completed in 2006 and validation continued in 2007

Briefly, to identify new genes that regulate cell motility we screened the human kinase, phosphatase and a custom migration siRNA library (termed MAR for migration and adhesion related) using a high throughput wound healing assay. We identified genes that accelerated (101 genes) or impaired migration (202) and a sub-set that induced impaired migration with an associated effect on viability, metabolism or loss of cell-cell/cell-substratum adhesion (154).

### *Validation of the SMARTpool screen*

We validated the SMARTpool phenotype for all 3 libraries by screening 2 of the 4 individual siRNA sequences. These data made us realise we couldn't have high confidence in the phenotype by just screening 2 sequences (this was the number originally thought in the field to be sufficient). Therefore, we focused in greater detail on the genes that Accelerated migration and screened all 4 siRNA sequences (finished end of 2006). This successfully defined a High Confidence (HC) sub-set of genes such that during 2007 we chose to do the same for the genes that Impaired migration (154 siRNAs). We also screened the HC Accelerated migration siRNAs with a different siRNA reagent (marketed to reduce off target effects), called ON-TARGET<sub>plus</sub>. These data gave further confidence to the existing HC data and also allowed us to promote several genes that had previously scored with Moderate Confidence. In summary we identified 66 HC genes, 34 that Accelerate migration and 32 that Impair migration. For a summation of the screening data and validation see Figure 1. We have subsequently focused on these HC genes in greater detail as outlined below.

*Aim 4.3- collate data from all screens, segregate into functional categories and analyse the data for pathway linkages using bioinformatics approaches.*

Ongoing from 2006 through 2007.

We took a range of approaches to informatically mine the screen data. We searched several independent databases (NIH DAVID, Bioknowledge library, Gene Sifter) using broad gene ontology terms related to the biological process of migration; including ‘cell migration, cell adhesion, cell-cell adhesion and cell-substrate adhesion’ and terms related to the cellular components; ‘actin cytoskeleton, lamellipodium, focal adhesion and adherens junction’. This allowed us to identify 42 HC genes (22 Accelerated and 20 Impaired) that have no prior association with cell migration or adhesion. Perhaps even more exciting, 12 of these genes had no experimentally supported Gene Ontology annotation in the BIOBASE database, making them truly interesting as they are not only uncharacterised but also have strong roles in migration. These genes are ripe for future study.

To investigate the signalling pathways regulating motility in MCF-10A cells we used Ingenuity software and queried the network linkages of the genes in the Accelerated, Impaired and Low Alamar bins. Together, the Accelerated and Impaired HC siRNAs work predominantly through 3 major signalling hubs,  $\beta$ -catenin, Actin and  $\beta$ 1-integrin (Figure 2). The Low Alamar signalling network centres on the critical tyrosine kinase EGFR.  $\beta$ -catenin regulates cell adhesion through its interaction with classic cadherins and other junctional proteins, but also mediates pleiotrophic changes in cell behaviour through its activity as a nuclear transcription regulator (Brembeck *et al.*, 2006). Many of the genes interacting with  $\beta$ -catenin caused cell-cell dissociation from the epithelial sheet, supporting a role for these genes in regulating cell-cell adhesion in MCF10A cells. Conversely, the Integrin and Actin networks were enriched in genes that Impaired cell migration. Integrin  $\beta$ 1 interacts with genes regulating focal adhesions. We created an annotated list of genes that are involved in  $\beta$ 1 and focal adhesion signalling based on our informatics and the focal adhesion genes annotated in the Adhesome (Zaidel-Bar *et al.*, 2007). Enrichment of Actin interactive proteins was expected given their critical role in regulation of the cytoskeleton and motility, thus the identification of this hub is confirmation of the screen but in addition, we identified a number of genes involved in this network that have had previously been linked with the actin cytoskeleton. In summary, we conclude these networks are integral to cell migration in MCF-10A cells with the screen adding valuable new gene associations to these signalling proteins.

*Aim 4.4 Develop tertiary assays to further subdivide functional categories and follow up critical candidates at a biochemical level.*

In 2006 I attempted to set up high throughput time-lapse video microscopy in the 96 well screening format. For a number of technical reasons this proved too difficult. In response to reviewers comments, we scaled the transfection conditions to 24 well dishes (avoiding the technical issues of using a 96 well plate) and under phase contrast conditions, imaged the 66 HC Accelerated and Impaired migration siRNAs by time-lapse. These data are all available on the Migration Consortium website and are described in more detail below. Control cells move as an epithelial sheet, maintaining adhesive contacts in a fashion termed ‘collective migration’, similar to that observed for Madin Darby Kidney epithelial cells (MDCK) (Poujade *et al.*, 2007). Comparing the migration phenotypes within the Accelerated and Impaired bins against the pattern of migration for Control cells allowed us to bin the genes into sub-classes of migration based on a core set of migration parameters (cell-cell adhesion, migration pattern, lamellipodia formation, speed, shape, net distance migrated). It was clear from these movies that accelerated migration is associated with a reduction in cell-cell adhesion, with 13 of the 34 siRNAs dramatically reducing cell contact concomitant with very fast and highly erratic motility (Table 1). Two other siRNAs caused complete loss of cell-cell contact and another two induced weak and transient adhesions. The remaining siRNAs accelerated migration but maintained monolayer integrity and were differentiated by the size of the lamellipodia. A representative from each of these groups was chosen and

the migration pattern traced for 8 independent cells. Graphing the pattern for a single cell showed that the genes that belonged to Group C (minimal adhesion, erratic migration, poor or non-existent front-rear polarity) were much faster and despite closing the wound, highly random in the direction of motility (Figure 3). We observed fewer distinguishing migration features for the siRNAs that impaired migration, with 18 of the 32 siRNAs reducing motility speed in a manner that morphologically indistinguishable from controls, although lamellipodia size varied to some extent. A number of siRNAs induced significant random motility within the monolayer but no actual forward movement to fill the cleared space, suggesting migration was impaired by the leading, wounded cells being unable to generate polarity or traction to move to the cleared space. Loss of ACTB (actin) expression resulted in a dramatic phenotype in which lamellipodia formation was essentially absent and cells moved very slowly with a smooth and united front. Formation of lamellipodia at the wound edge is necessary to facilitate cell movement and is predominantly a RAC1 driven process in fibroblasts and MDCK cells (Charest and Firtel, 2007). As anticipated, we generally observed limited lamellipodia formation for the siRNAs that impaired migration suggesting many of these genes regulate migration at the level of actinomyosin contraction and polymerisation. In contrast we found that a wide range of lamellipodia size can result in increased migration, not simply large protrusive lamellipodia as shown previously for fibroblasts (Vincente-Manzanares et al., 2007), directly implicating a role for many of these genes in myosin polymerisation dynamics. A number of siRNAs caused defects in cell polarity, suggesting known regulators of polarity, including TIAM1 or CDC42 may be downstream targets (Pegtel et al., 2007; Charest and Firtel, 2007). Further biochemical analysis is required to confirm these speculations.

We validated 20 candidate siRNAs by shRNA knockdown (Open Biosystems), permitting longer-term assays due to the stability of knockdown. All showed 1 or more shRNA sequences that replicated the wound healing phenotype. We are continuing to generate cell lines to complete all the genes in the HC Accelerated group. This will allow extensive tertiary screening using model assay systems that more closely reflect the tumourigenic potential of cell lines and permit them to be performed in parallel as cell number will no longer be limiting. These assays include Boyden chamber invasion assays, morphology in 3D, growth factor independence, transformation potential in soft agar and ultimately tumourigenicity *in vivo*. These approaches will allow us to extrapolate the screening data to the greater relevance of breast carcinoma.

#### *Aim 4.5 – identify genes that interact with RHOA and RHOC.*

In the interest of remaining focused on publishing the manuscript and addressing reviewers comments this Aim was not pursued.

#### *Additional*

As part of our involvement in the Cell Migration Consortium we committed to make all the screening data publicly available. This sets our screen aside from typical screens in which a one or several candidates (not necessarily those that are the top hits) are followed in great detail while the remainder of the screening data remains essentially buried. We created a fully interactive database hosted by the Consortium with a gateway through Nature that allows researchers to search any of the screening parameters (Figure 4), visualise a representative wound and associated higher resolution morphology (Figure 5) and view the time-lapse migration pattern of the siRNA alongside the control (Figure 6). All the migration parameters defined by the time-lapse are included on a single page, together with a time-course of static images collated over the 20 hours of imaging. The website will not be made public until published, screen shots are shown for Figures 4, 5 and 6.

### **Key Research accomplishments**

- Identified 34 High Confidence siRNAs that Accelerate migration
- Identified 32 High Confidence siRNAs that Impair migration
- Characterised the migration pattern of these 66 HC siRNAs by time-lapse video microscopy
  - Binned the siRNAs into common morphological/migratory features
  - Identified loss of cell-cell contact as a major mechanism for cell motility
  - Identified a very interesting subset that accelerate migration without losing cell-cell contact
- Identified 3 major signalling hubs that regulate motility in MCF-10A cells, at least in 2D
  - $\beta$ -catenin,  $\beta$ 1-integrin and actin
- Generated stable knockdown cell lines for key candidate Accelerated migration genes using a lentiviral shRNA approach
  - Validated wound healing phenotype for these lines
- Documented the entire screen, validation, secondary screen and time-lapse imaging on a publicly available website.

### **Reportable outcomes**

#### Publications

Melani M, Simpson KJ, Brugge JS and Montell D. Regulation of cell adhesion and collective cell migration by Hindsight and its human homolog RREB1. In Press: *Current Biology*.

Simpson KJ, Selfors LM, Bui J, Reynolds A, Leake D, Khvorova A and Brugge JS. Identification of genes that regulate epithelial cell migration using an siRNA screening approach. Under review at *Nature Cell Biology*. Manuscript will be submitted with final report.

Simpson KJ, Selfors LM, Bui J, Reynolds A, Leake D and Brugge JS. Acceleration and suppression of human epithelial cell migration using a high throughput siRNA approach. In: Breast Cancer Research at Harvard. Transactions of the 4th Symposium, March 23, 2007. \*Included invited Oral presentation.

#### Oral presentations

4th Annual Dana Farber/Harvard Cancer Centre program in breast cancer. Boston, Massachusetts, USA. Acceleration and suppression of human epithelial cell migration using a high throughput siRNA approach. March 23.

RNAi Global Meeting. Denver, Colorado, USA. Acceleration and suppression of epithelial cell migration using a high throughput siRNA screening approach. April 12.

Breast Cancer Program Project Grant (to Drs J Brugge, R Weinberg, D Livingston, M Brown, J Labaer, M Ewen, K Polyak) Annual retreat. Colerain, Massachusetts, USA. Identifying genes that regulate cell migration using an siRNA screening approach. May 14.

Cell Migration Consortium Annual meeting. Reston, Virginia, USA. Identification of genes that regulate epithelial cell migration using an siRNA screening approach. September 28.

#### Training

- Full time supervision of a technical assistant

- Supervision of a rotating Graduate student
- Manuscript revisions both independently and in conjunction with Dr. Brugge
- Preparation of the annual report and grant renewal for our contribution to the Cell Migration Consortium NIH glue grant

#### Current collaborations

Dr. Devin Leake and Angela Reynolds, Thermo Fisher (Dharmacon RNA technologies). Quantitation of siRNA knockdown using a high throughput screening approach.

Dr Denise Montell and Dr Mariana Melani, Johns Hopkins School of Medicine, Baltimore. Analysis of the human homologs that have a migration defect identified in *Drosophila*.

#### General comments

A no-cost extension was granted to this award that allowed the completion of the manuscript. The manuscript was under initial review at Nature Cell Biology for 7 weeks and reviewers were extremely positive about the integrity of the screen and subsequent analysis. More data was requested, primarily in the form of time-lapse imaging and while this was technically challenging, it seemed inappropriate from our perspective to analyse only a small subset of genes (as requested). Indeed at its conclusion, this analysis has proved extremely informative and we are hopeful that our re-submission (planned in approximately 10 days) will be received favourably. Some of the data generated in this past year was used to gain NIH funding as we are members of the Gene Expression group of the Cell Migration Consortium.

#### **Conclusions**

We have identified a number of candidate genes that either positively or negatively regulate epithelial cell migration. Through time-lapse videomicroscopy we have identified a number of genes that regulate cell-cell adhesion, with loss of expression of these genes resulting in highly motile cells. These represent potentially novel tumour suppressor genes. Stable cell lines are currently being generated to allow more detailed analyses and further insight into the mechanisms regulating the migratory phenotype with a view to extrapolating to invasive breast carcinoma.

#### **References**

Brembeck F.H, Roasario M and Birchmeir W. Balancing cell adhesion and Wnt signalling, the key role of beta-catenin. *Curr. Opin. Genet. Dev.* 16:51-59, 2006.

Zaidel-Bar R, Itzkovitz S, Ma'ayan A, Iyengar R and Geiger B. Functional atlas of the integrin adhesome. *Nat. Cell Biol.* 9:858-867, 2007.

Poujade M, Grasland-Mongrain E, Hertzog A, Jouanneau J, Chavrier P, Ladoux B, Buguin A and Silberzan, P. Collective migration of an epithelial monolayer in response to a model wound. *Proc. Natl. Acad. Sci. USA* 104:15988-15993, 2007.

Charest PG and Firtel RA. Big roles for small GTPases in the control of directed cell movement. *Biochem. J.* 401:377-390, 2007.

Vincente-Manzanares M, Zareno J, Whitmore L, Choi CK and Horwitz AF. Regulation of protrusion, adhesion dynamics and polarity by myosins IIA And IIB in migrating cells. *J. Cell Biol.* 176:573-580, 2007.

Pegtél DM, Ellenbroek SI, Mertens AE, van der Kammen RA, de Rooij J and Collard JG. The Par-Tiam1 complex controls persistent migration by stabilising microtubule-dependent front-rear polarity. *Curr. Biol.* 17:1623-1634, 2007.

## **Appendices**

Melani et al., Current Biology manuscript

## **Supporting data**

Figure 1: Schematic of the *SMART*pool screen and validation screens.

Figure 2: Top signalling network of direct relationships for the HC Accelerated and Impaired genes.

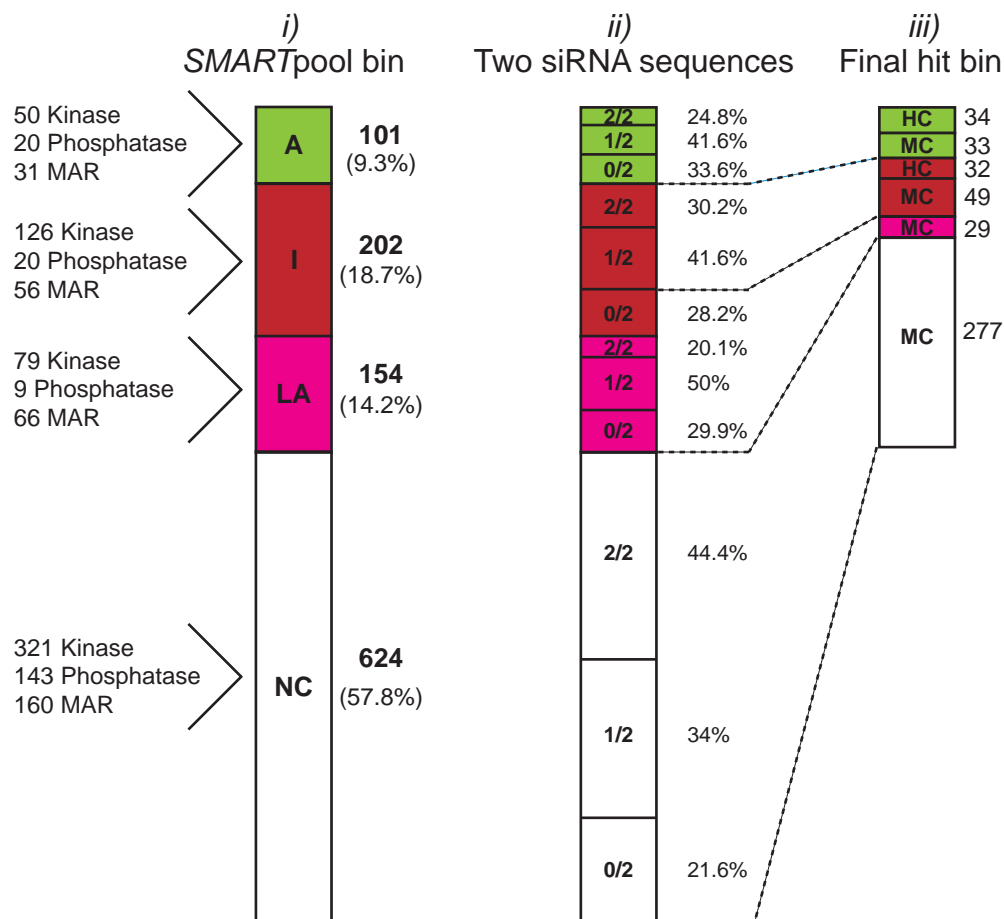
Figure 3: Analysis of the migration pattern of individual cells from representative HC Accelerated genes determined by time-lapse imaging.

Figure 4: A screen shot of the opening page of the siRNA screening data.

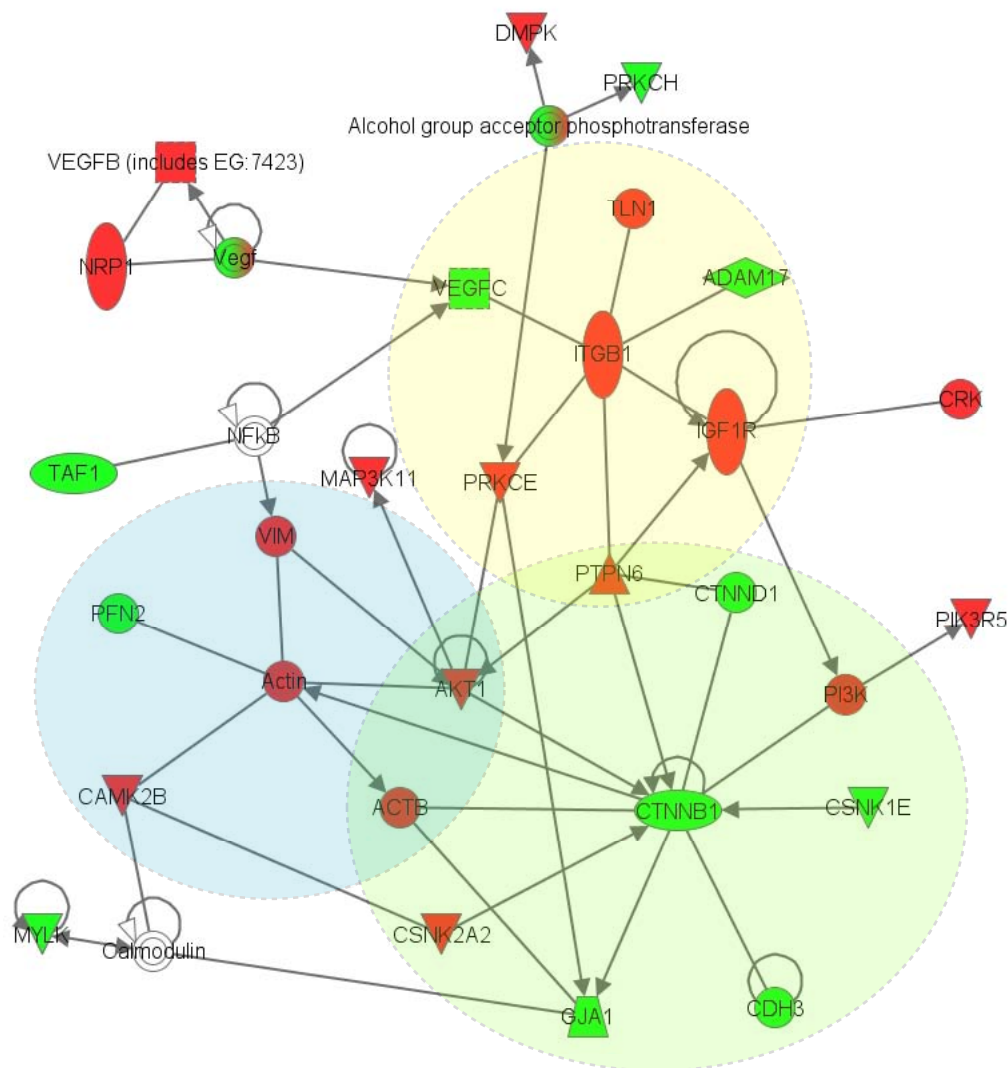
Figure 5: Screen shot of the linked pages that show a representative wound relative to control and the associated morphology.

Figure 6: Screen shot of the time-lapse migration page for a representative gene.

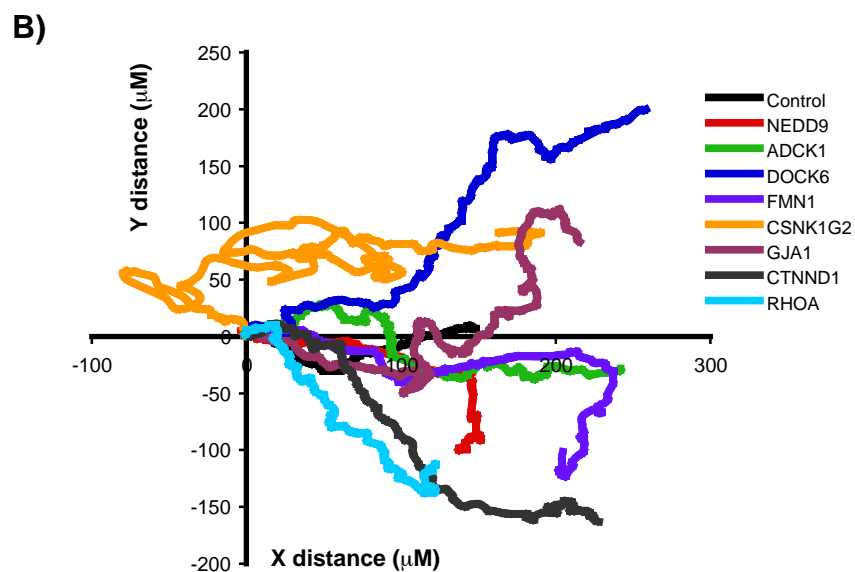
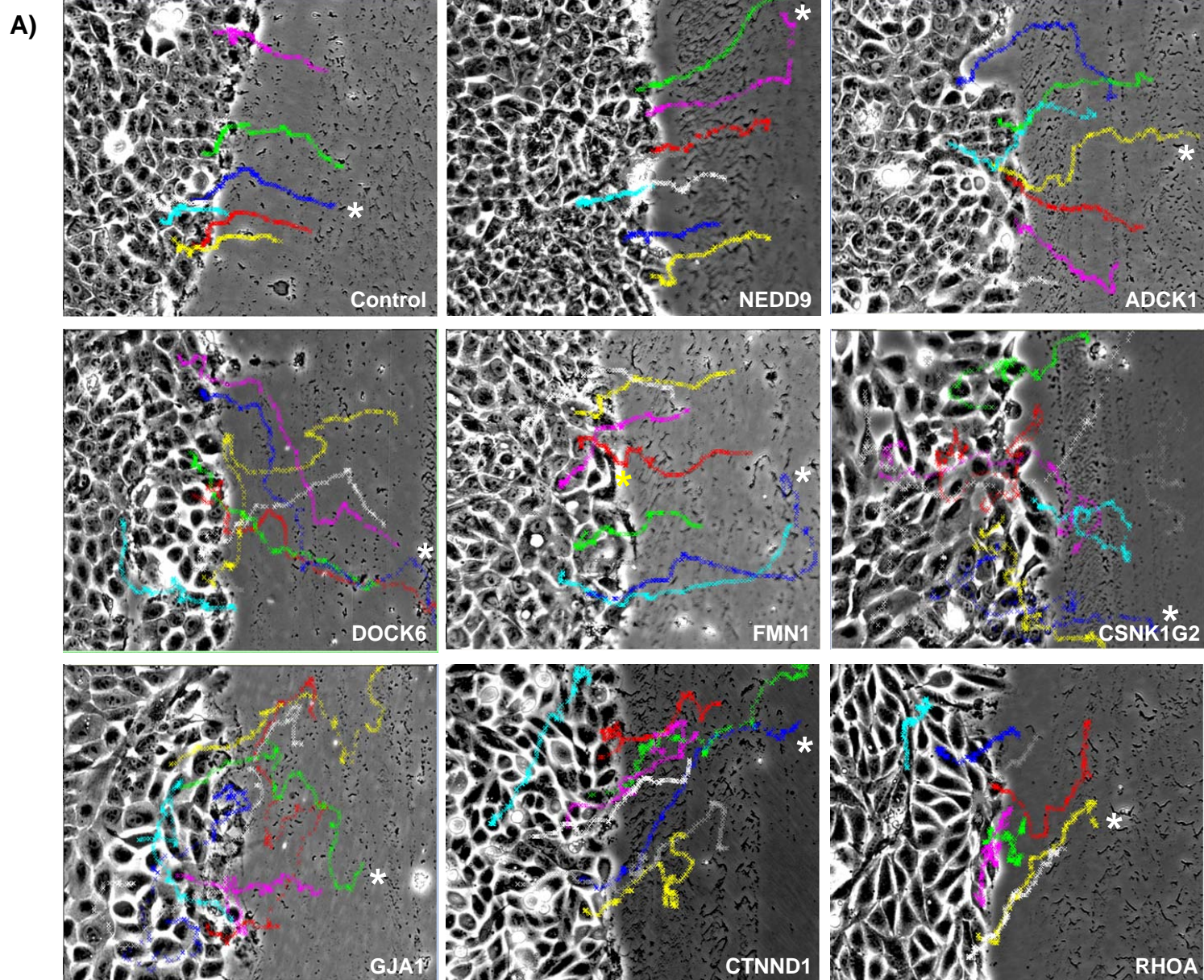
Table 1: Classification of the Accelerated and Impaired genes by time-lapse video microscopy.



**Figure 1:** Schematic of the *SMARTpool* screen and validation screens. i) On the left, the contribution of each library (Kinase, Phosphatase or Migration and Adhesion related (MAR) to each hit bin; Accelerated migration (A), Impaired migration (I), Low Alamar (LA) and No Change (NC). On the right, the total number of siRNAs in each hit bin and the relative proportion of the entire screen. ii) Distribution of the phenotypic concordance of the two siRNAs sequences within each hit bin and expressed as a proportion of the total number of siRNAs in each bin. A score of 2/2 means both sequences agreed with the *SMARTpool*. iii) Final hit distribution after collation of individual sequence siRNA and ON-TARGET*plus* siRNA reagent validation. HC= high confidence, MC= moderate confidence, indicated in absolute numbers.



**Figure 2:** Top signalling network of direct relationships for the HC Accelerated and Impaired genes. Ingenuity pathway analysis of the 66 genes identified direction interactions between 27 genes within one network. This indicates the major signalling hubs important for cell migration (defined as genes with greater than 5 interacting partners) centre around  $\beta$ -catenin (shaded green),  $\beta$ 1-integrin (shaded yellow) and Actin (shaded blue). KEY: green=Accelerated, red=Impaired, white=other interacting proteins that if screened did not give a phenotype, diamond=enzyme, circle=other, triangle=kinase, rectangle=GPCR, vertical oval=transmembrane receptor, horizontal oval=transcription regulator, square=growth factor, pentagon=transporter. A dilled arrow indicates the direction of the interaction, an open arrow indicates translocation.



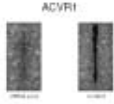
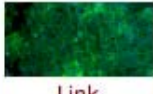

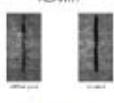
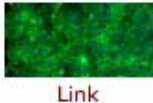




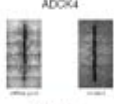
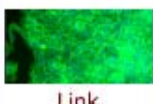

**Figure 3:** Analysis of the migration pattern of individual cells from representative HC Accelerated genes determined by time-lapse imaging. Cells moved from left to right, the first frame is shown in (A). The paths of 8 cells (coloured) were traced for 201 frames (every 6 mins for 20 hours). The cell paths indicated by \* are graphed in (B) which represents the X- and Y-axis migration ( $\mu\text{M}$ ).

[Download Excel Spreadsheet](#)

Search by:

Sort by:  Show:

ascending / descending   [Reset](#)

siRNA Migration Screen						
	Gene	Description <sup>1</sup>	MCF-10A phenotype <sup>2</sup>	Secondary screen <sup>3</sup>	Wound <sup>4</sup> Image	Morphology <sup>5</sup> Time-lapse <sup>6</sup>
1	<a href="#">ACVR1</a> Aliases: FOP, ALK2, SKR1, ACTR1, ACVRLK2 Entrez Gene: <a href="#">90</a> <a href="#">siRNA catalog</a>	<b>activin A receptor, type I</b> mRNA: <a href="#">NM_001105</a> Library: <b>Kinase</b> Classification: <b>Ser/Thr Kinase</b>	Final bin: <b>Accelerated - HC</b> SMARTpool bin: <b>Accelerated</b> Avg area: <b>0.18</b> Avg Alamar: <b>1.03</b> Knockdown %: <b>80-90</b>	ERBB2: <b>Accelerated</b>	 <a href="#">Link</a>	 <a href="#">Link</a> <b>Accelerated unique</b>  <a href="#">Link</a>
2	<a href="#">ADAM17</a> Aliases: TACE, cSVP, CD156b Entrez Gene: <a href="#">6868</a> <a href="#">siRNA catalog</a>	<b>ADAM metalloproteinase domain 17 (tumor necrosis factor, alpha, converting enzyme)</b> mRNA: <a href="#">NM_003183</a> Library: <b>MAR</b> Classification: <b>metalloproteinase</b>	Final bin: <b>Accelerated - HC</b> SMARTpool bin: <b>Accelerated</b> Avg area: <b>0.65</b> Avg Alamar: <b>0.97</b> Knockdown %: <b>not done</b> ON-TARGETplus: <b>No Change</b>	ERBB2: <b>Accelerated</b>	 <a href="#">Link</a>	 <a href="#">Link</a> <b>Accelerated E</b>  <a href="#">Link</a>
3	<a href="#">ADCK1</a> Entrez Gene: <a href="#">57143</a> <a href="#">siRNA catalog</a>	<b>aarF domain containing kinase 1</b> mRNA: <a href="#">NM_020421</a> Library: <b>Kinase</b> Classification: <b>Ser/Thr Kinase</b>	Final bin: <b>Accelerated - HC</b> SMARTpool bin: <b>Accelerated</b> Avg area: <b>0.36</b> Avg Alamar: <b>1.05</b> Knockdown %: <b>failed</b> ON-TARGETplus: <b>Accelerated</b>	ERBB2: <b>Accelerated</b>	 <a href="#">Link</a>	 <a href="#">Link</a> <b>Accelerated E</b>  <a href="#">Link</a>
4	<a href="#">ADCK4</a> Aliases: COQ8 Entrez Gene: <a href="#">79934</a> <a href="#">siRNA catalog</a>	<b>aarF domain containing kinase 4</b> mRNA: <a href="#">NM_024876</a> Library: <b>Kinase</b> Classification: <b>Ser/Thr Kinase</b>	Final bin: <b>Accelerated - HC</b> SMARTpool bin: <b>Accelerated *</b> Avg area: <b>0.84</b> Avg Alamar: <b>0.95</b> Knockdown %: <b>80-90</b> ON-TARGETplus: <b>Accelerated</b>	ERBB2: <b>No Change</b>	 <a href="#">Link</a>	 <a href="#">Link</a> <b>Accelerated C</b>  <a href="#">Link</a>

**Figure 4:** A screen shot of the opening page of the siRNA screening data. The entire screen can be searched on any of the parameters listed in the detailed columns and then sorted to refine the list. Shown above, the dataset has been interrogated to show all the genes that accelerated migration and were analysed by time-lapse video microscopy. The Gene is hyperlinked to a second Migration Consortium page with detailed information on the gene and family members. Links to Entrez gene are included. The siRNA catalog link provides users the catalog of the SMARTpool and all 4 individual siRNAs used and whether they scored in the screen. The library of origin and classification of the gene family is included. The MCF-10A phenotype column details all the screening data; Final bin after validation, original screen bin (SMARTpool bin), average wound healing area score, average alamar blue score, the extent of knockdown (if analysed) and the phenotype after screening using ON-TARGETplus reagents (if analysed). Secondary screening in additional cell lines was performed and the phenotype is annotated in this column. The remaining columns show a thumbnail of the wound, morphology and a static progression of the time-lapse microscopy data. These columns all hyperlink to additional pages with higher resolution images, more detailed information and the time-lapse movies. These are shown in greater detail in Figures 6 and 7. The complete dataset can also be downloaded.

A)

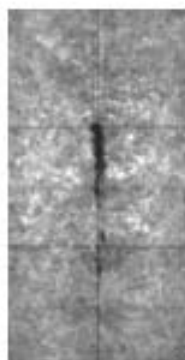
### Representative Wound :

[ADCK1](#) aarF domain containing kinase 1

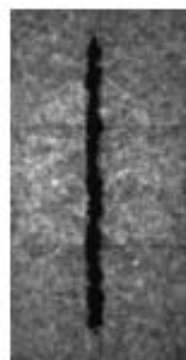
Final bin: Accelerated - HC

Library: Kinase

ADCK1



siRNA pool



Control

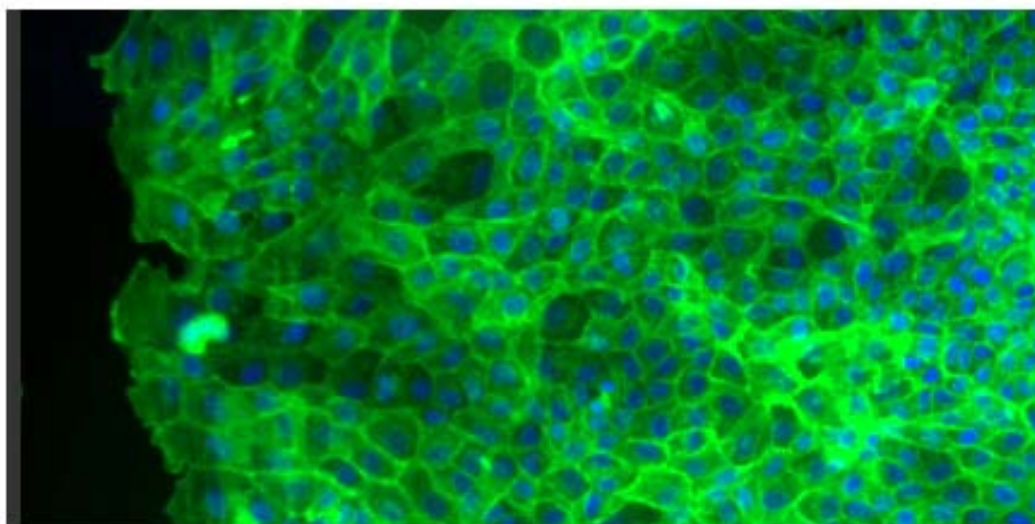
B)

### Representative Morphology :

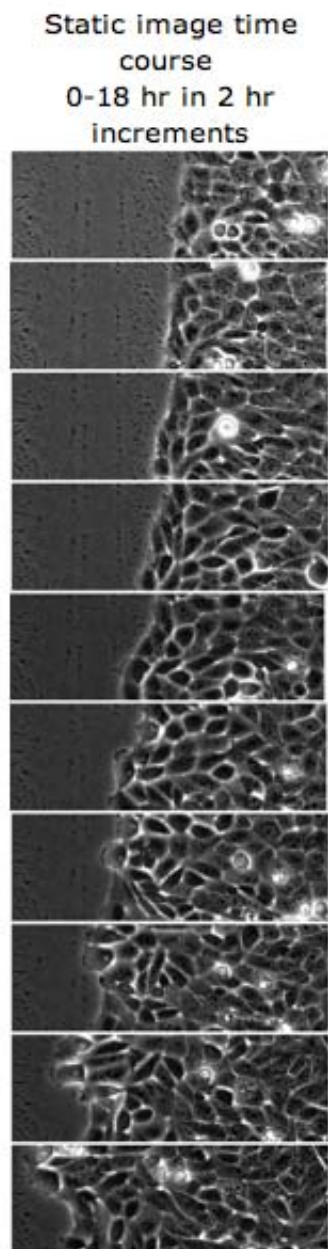
[ADCK1](#) aarF domain containing kinase 1

Final bin: Accelerated - HC

Library: Kinase



**Figure 5:** Screen shot of the linked pages that show a representative wound relative to control and the associated morphology (separate link). The final hit bin and library of origin are indicated. The gene name is hyperlinked to a page containing a detailed description of the gene and family members that is curated by the Cell Migration Consortium.



## ADCK1

[NM\\_020421](#)

aarF domain containing kinase 1

**Accelerated - HC**

**Group E- adhesive, collective, medium lamellipodia**

### *Migration characteristics\**

Adhesion: +++

Migration: **Directed, collective**

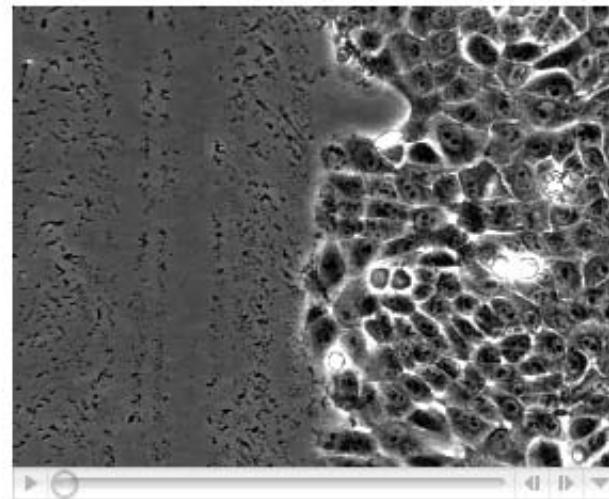
Shape: **Epithelial**

Speed: ++

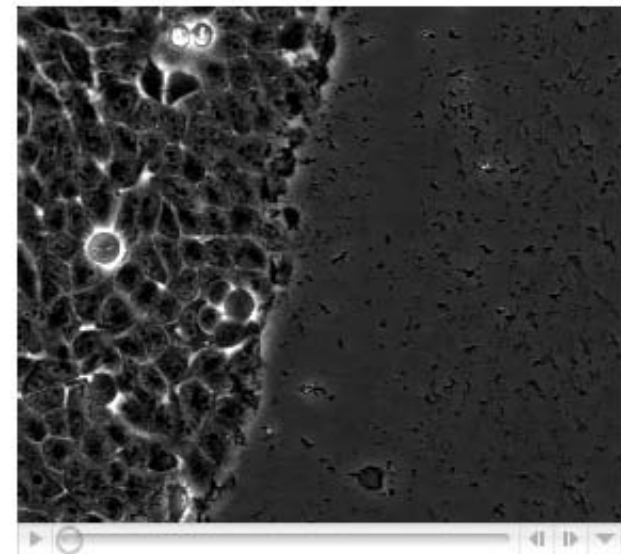
Lamellipodia formation: **Small, edge only**

\*[Key](#) for time-lapse phenotypes

**siRNA:**



**Control:**



**Figure 6:** Screen shot of the time-lapse migration page for a representative gene. All the characteristics listed are included as a Supplementary Table in the manuscript. The static time course offers a snap shot of the migration progression and morphology features if the user did not choose to play the movies. Movies are embedded and can be played simultaneously for a direct comparison to control. A key is provided as a link to explain the migration characteristics.

**Regulation of cell adhesion and collective cell migration by Hindsight and its  
human homolog RREB1**

Mariana Melani<sup>1</sup>, Kaylene Simpson<sup>2</sup>, Joan Brugge<sup>2</sup> and Denise Montell<sup>1,3</sup>

HNT and RREB1 control collective cell movement and adhesion

<sup>1</sup>Department of Biological Chemistry

Johns Hopkins University School of Medicine

725 North Wolfe Street, Baltimore, MD 21205, USA

<sup>2</sup>Department of Cell Biology

Harvard Medical School

240 Longwood Avenue, Boston, MA 02115, USA

<sup>3</sup>Corresponding author

Phone (410) 614-2016; Fax (410) 614-8375

[dmontell@jhmi.edu](mailto:dmontell@jhmi.edu)

## Summary

Cell movements represent a major driving force in embryonic development, tissue repair and tumor metastasis [1]. The migration of single cells has been well-studied, predominantly in cell culture [2, 3]; however *in vivo*, a greater variety of modes of cell movement occur, including the movements of cells in clusters, strands, sheets and tubes, also known as collective cell migrations [4, 5]. In spite of the relevance of these types of movements in both normal and pathological conditions, the molecular mechanisms that control them remain largely unknown. Epithelial follicle cells of the *Drosophila* ovary undergo several dynamic morphological changes, providing a genetically tractable model [6]. We found that anterior follicle cells, including border cells, mutant for the gene *hindsight (hnt)* accumulated excess cell-cell adhesion molecules and failed to undergo their normal collective movements. In addition, HNT affected border cell cluster cohesion and motility via effects on the JNK and STAT pathways, respectively. Interestingly, reduction of expression of the mammalian homolog of HNT, RREB1, by siRNA inhibited collective cell migration in a scratch-wound healing assay of MCF10A mammary epithelial cells, suppressed surface activity, retarded cell spreading after plating and led to the formation of immobile, tightly-adherent cell colonies. We propose that HNT and RREB1 are essential to reduce cell-cell adhesion when epithelial cells within an interconnected group undergo dynamic changes in cell shape.

## Results and Discussion

### ***hnt* controls morphogenetic changes through the regulation of adhesion molecules**

A variety of epithelial cell rearrangements occur during the normal development of *Drosophila* egg chambers, which are composed of approximately 650 follicular epithelial cells surrounding 15 nurse cells and one oocyte (Figure 1A). Initially all of the follicle cells are cuboidal in shape and adhere to each other through adherens junctions which contain *Drosophila* E-cadherin (DE-CAD), N-cadherin (DN-CAD) and  $\beta$ -catenin (Armadillo, ARM) (Figure 1A-A' and data not shown). These cell-cell contacts are extensively remodeled as egg chamber development progresses (reviewed in [6]). Between 50 and 100 anterior follicle cells, known as “stretched follicle cells”, transform from cuboidal to squamous, expanding the apical and basal domains while shrinking the lateral membrane (Figure 1A'-D', insets), a process that is accompanied by a dramatic down-regulation of DE-CAD, DN-CAD and ARM at the plasma membrane (Figure 1A'-D' and data not shown). This leads to a decrease in follicle cell density in the anterior half of the egg chamber (Figure 1A'-D', insets). In contrast, stretched follicle cells mutant for *hnt* retained abnormally high levels of ARM at the membrane (Figure 1E, E') and the cell density in mutant clones was 3.5 times higher than equivalent wild type areas, indicating that the mutant cells failed to spread. DN-CAD expression was also elevated in *hnt* mutant clones, even for a single mutant cell at an early stage of development, in which the overall cell size and shape were similar to neighboring wild-type cells (Figure 1F-F'''). These observations suggest that HNT regulates the cell shape changes of the stretched follicle cells via its effect on the accumulation of cell-cell

adhesion molecules. Consistent with this interpretation, previous work has shown that loss of *arm* alone is sufficient to cause early stage follicle cells that are normally cuboidal to assume a flattened, squamous morphology [7].

At the same time that the stretched follicle cells flatten, the vast majority of the follicle cells, the “main body follicle cells”, change their morphology from cuboidal to columnar (Figure 1A'-D'). When mutant for *hnt* they also exhibited an accumulation of ARM and DE-CAD (Figure 1G-H'). We quantified the levels of ARM and DE-CAD and found a 2 fold enrichment in *hnt* mutant cells over wild type neighbors (Figure S1A). Since ARM and DE-CAD always co-localized in follicle cells (Figure 1A-D), we used them interchangeably through the rest of this study.

Several other adhesion proteins (DN-CAD, FASIII and FASII) were also enriched in the plasma membrane of *hnt* mutant cells (Figure 1I-J' and not shown). The effects appeared to be specific for cell adhesion molecules, because the transmembrane receptor tyrosine kinases PVR and DER were not enriched in the mutant cells (not shown), nor was the distribution of cortical F-actin altered (Figure 1K-K'). In spite of the accumulation of adhesion proteins, we did not observe any morphological defects in *hnt* mutant main body follicle cells, suggesting that the cuboidal to columnar cell shape change is compatible with increased lateral cell-cell adhesion. Together these results indicate that *hnt* is required to down-regulate the levels of adhesion proteins in cells that change shape by reducing, but not eliminating, lateral cell-cell adhesion. The need to retain some cell-cell adhesion while moving is a defining feature of collective cell migration.

### ***hnt* is required for collective migration of the border cells**

Another sort of collective movement that takes place during *Drosophila* oogenesis is the migration of the border cells (Figure 1 and 2A). The border cells are a population of 4-6 follicle cells that cluster around a pair of polar cells, delaminate from the anterior follicular epithelium (Figure 1B) and migrate in between the nurse cells (Figure 1C), reaching the oocyte by stage 10 (Figure 1D, 2A). Clusters composed entirely of *hnt* mutant border cells failed to initiate migration and stayed at the anterior tip of the egg chamber (Figure 2B; n>17) and appeared more compact than wild type clusters (Figure 2B compared to 1B, inset).

Border cell migration requires complex regulation of cell-cell adhesion because they must detach from the anterior follicle cells while remaining adherent to each other and to the polar cells. Meanwhile, they have to both attach to and detach from the nurse cells repeatedly as they move. In wild-type clusters, DE-CAD and ARM accumulate to highest levels at the interface between the border cells and the polar cells, which are located at the center of the cluster [8, 9] (Figure 2A, C). In contrast, in *hnt* mutant clusters DE-CAD and ARM accumulated more uniformly (Figure 2B, E-F and not shown). We performed a detailed analysis of the levels of ARM in wild type and in mosaic clusters composed of mixtures of mutant and wild-type cells (Figure 2C,C',E,E'). A line scan across the center of a wild type border cell cluster, confirmed the higher concentration of ARM at the border cell/polar cell interface (Figure 2D). This type of analysis revealed that in *hnt* mutant border cells, ARM was enriched to levels normally found in the polar cells (Figure 2F).

HNT is a Zinc finger-containing transcription factor that has previously been shown to be required for several morphological changes that occur during embryogenesis [10-12]. We examined the HNT expression pattern in stage 9 and 10 egg chambers and found that it was most highly expressed in the stretched follicle cells and border cells (Figure 2A). HNT was also expressed but at a lower level in the main body follicle cells and was undetectable in the polar cells and stalk cells (follicle cells that connect adjacent egg chambers). These expression levels correlate with the extent of the morphological changes that the different cell populations undertake.

### **HNT over-expression leads to cluster disassembly and inhibition of migration**

HNT also caused a striking gain-of-function phenotype when over-expressed in the border cells. In control egg chambers, 90% of the border cell clusters completed migration by early stage 10 (Figures 3A, I and Movie S1) and exhibited a typical rosette morphology (Figure 3B). Border cell clusters over-expressing *hnt* exhibited dramatic changes in motility, morphology, and cluster cohesion (Figures 3C-D and Movie S2). The border cells were markedly elongated and splayed apart, though they remained attached to the polar cells. We quantified the dissociation phenotype by measuring the radius of the border cell cluster. In wild-type, the cluster radius averaged 13 $\mu$ m whereas clusters over-expressing *hnt* had an average radius of 43  $\mu$ m (Figure 3I). These disassembled clusters failed to complete migration in 100% of stage 10 egg chambers (Figures 3C, I). We took advantage of the FLP-OUT technique [13] to over-express *hnt* in random subsets of cells, in order to examine the levels of adhesion proteins in border cells with elevated levels of *hnt*. We found that ARM levels were 2

fold reduced in HNT over-expressing (GFP positive) cells compared to wild type (GFP negative) cells in the same cluster (Figure S1B and S2A). The same reduction was observed for DE-CAD (not shown) but not for Singed (SN, *Drosophila* fascin), aPKC or F-actin (Figure S2B-D).

The cluster disassembly phenotype caused by excess levels of HNT was completely rescued by simultaneous over-expression of *arm* or *shotgun* (DE-CAD), whereas we observed only a partial rescue of the migration phenotype under the same conditions (Figure 3I and not shown). These observations indicate that cohesion among the members of the migratory group and motility are separable features of this type collective cell migration, which are both affected by HNT.

### **The effects of HNT on border cell cluster cohesion and motility are mediated by the JNK and STAT pathways, respectively**

To explore the mechanisms by which HNT affects cluster cohesion and motility, we investigated its effects on known signaling pathways. In the extra-embryonic tissue known as the amnioserosa, *hnt* is a negative regulator of the JNK signaling cascade [12]. Recently, the JNK pathway was shown to be active in the border cells and to affect border cell migration in clusters with reduced PVR activity [14]. In addition, inhibition of the JNK cascade causes a phenotype that strikingly resembles the cluster dissociation phenotype caused by HNT over-expression (Llense et al., personal communication), suggesting that HNT could be a negative regulator of the JNK pathway or vice versa. Using phospho-JUN antibody staining as a readout of the JNK signaling cascade, we detected that the activity of this pathway was reduced in border cells over-

expressing *hnt* (Figures 3E, F). In clusters in which JNK was reduced by over-expression of either *puckered* (the JNK phosphatase) or a dominant-negative form of *basket* (*Drosophila* JNK), cluster disassembly reminiscent of the *hnt* gain-of-function phenotype was observed (Figure 3G-I, not shown and Lense et al). In addition, HNT was up-regulated 1.7 and 1.4 fold, respectively (Figure 3G-H, inset and not shown). Together, these results indicate that *hnt* and JNK repress each other. In the embryo, where HNT also antagonizes JNK, this pathway is required for the turnover of focal complexes and proper dorsal closure [12]. Therefore HNT appears to play a general role in remodeling of adhesion complexes to facilitate morphogenesis.

While the cluster disassembly phenotype of HNT could be attributed to effects on JNK signaling, JNK pathway mutations caused milder border cell motility defects than *hnt* (Figure 3I, not shown and Lense et al). To determine if HNT affected, in addition, one of the known border cell motility pathways, we examined the effect of *hnt* on the activity of STAT and its key target SLBO. STAT activation and nuclear translocation is the most upstream event in the differentiation of the border cells and is also required throughout border cell migration [15, 16]. We found that, in border cells over-expressing HNT, nuclear accumulation of STAT was reduced though not eliminated (Figure S3B,C). In addition, the levels of SLBO were dramatically reduced in border cells over-expressing HNT (Figure S3D,E). Since loss of function of either STAT or SLBO causes a dramatic migration defect, the effects of HNT over-expression on STAT and SLBO can account for the severe effect on motility [16, 17]. However neither *stat* nor *slbo* mutant border cells exhibits a cluster disassembly phenotype. Therefore we conclude

that HNT mediates its effect on cluster cohesion via JNK and its effect on border cell motility primarily through STAT and SLBO.

Although HNT over-expression affects border cell motility via effects on STAT and SLBO, HNT has general effects on cell adhesion and morphogenesis whereas SLBO appears to be more specific. For example the effects of *hnt* on stretched follicle cells and in embryonic tissues are independent of SLBO since this protein is neither expressed nor required in these other cell types. Therefore we propose that HNT plays a general role in regulating cell adhesion and morphogenesis via JNK signaling and a tissue-specific role in motility through STAT and SLBO. In this way HNT can cooperate with tissue-specific factors to orchestrate a diverse array of collective cell movements.

### **The human homolog of HNT, RREB1, is required for spreading and migration of MCF-10A breast epithelial cells**

The human homolog of HNT is the Ras Responsive Element Binding Protein 1 (RREB1) (figure 4A) [10] [18]. Since HNT controls epithelial morphogenesis in several different tissues and stages of *Drosophila* development, we investigated whether RREB1 might function similarly in mammalian cells. Specifically, we investigated its role in the regulation of cell migration in the mammary epithelial cell line MCF-10A, using the classic scratch wound healing assay as a means of measuring collective migration in a monolayer [19]. In this assay, MCF-10A cells migrate as an epithelial sheet, retaining cell-cell adhesions during migration. We first knocked down expression of RREB1 using a *SMART*pool siRNA reagent, which contained four siRNAs complementary to different segments of the RREB1 mRNA. Cells transfected with the

RREB1 *SMART*pool showed a severe impairment of wound closure compared to the mock-transfected control cells (Figure 4B). We then tested the effect of each of the four individual siRNA constituents. Under the same assay conditions we found that three of the four individual siRNAs invoked a similar phenotypic response. Such strong phenotypic concordance provides high confidence for a role for RREB1 in regulating cell migration in MCF10A cells. In a high throughput screen of over 1,000 *SMART*pools such a severe phenotype was observed with high confidence for only 2.6% (KJS and JSB, manuscript submitted). In addition to inhibiting wound closure, we noticed that the RREB1 knockdown cells failed to form a complete monolayer, due at least in part to suppression of proliferation (KJS and JSB, unpublished) and not attributable to cell death as the phenotype that was not ameliorated by caspase inhibition (KJS and JSB, unpublished). Moreover, upon harvesting and replating, control MCF10A cells attach and spread rapidly, however the RREB1 knockdown cells while viable, formed aggregated clumps and spread poorly, then eventually generated tightly adherent epithelial islands (Figure 4C).

To study the migration defect further, we carried out live imaging analysis (Movies S3 and S4). Whereas control cells moved actively, making and breaking adhesive contacts with one another, RREB1 knockdown cells were strikingly immobile; there was a dramatic reduction in cell protrusions and lamellipodia and no evidence for dynamic cell-cell interactions. Western analysis showed a 25% increase in E-cadherin and  $\beta$ -catenin protein levels compared to the control (not shown). These findings strongly support our hypothesis that HNT and RREB1 play a conserved role in regulating dynamic changes in morphology, cell-cell adhesion, and collective migration

of epithelial cells in different tissues, developmental stages and organisms, as illustrated in Figure S4.

### **Acknowledgments**

We thank members of the fly community for reagents as listed on the text. We thank members of Denise Montell lab, specially Michelle Starz-Gaiano for helpful comments and discussion and Mohit Prasad for help with live imaging studies. We acknowledge James Bui for technical help. Thanks to Enrique Martin-Blanco for sharing unpublished data. The project described was supported by the Cell Migration Consortium Grant Number U54 GM064346, the Department of Defense (W81XWH-04-1-0360) and R01 GM73164 from the National Institute of General Medical Sciences. The content is solely the responsibility of the authors and does not necessarily represent the official views of the National Institute of General Medical Sciences or the National Institutes of Health.

## References

1. Franz, C.M., Jones, G.E., and Ridley, A.J. (2002). Cell migration in development and disease. *Dev Cell* 2, 153-158.
2. Ridley, A.J., Schwartz, M.A., Burridge, K., Firtel, R.A., Ginsberg, M.H., Borisy, G., Parsons, J.T., and Horwitz, A.R. (2003). Cell migration: integrating signals from front to back. *Science* 302, 1704-1709.
3. Vicente-Manzanares, M., Webb, D.J., and Horwitz, A.R. (2005). Cell migration at a glance. *J Cell Sci* 118, 4917-4919.
4. Friedl, P., Hegerfeldt, Y., and Tusch, M. (2004). Collective cell migration in morphogenesis and cancer. *Int J Dev Biol* 48, 441-449.
5. Rorth, P. (2007). Collective guidance of collective cell migration. *Trends Cell Biol* 17, 575-579.
6. Horne-Badovinac, S., and Bilder, D. (2005). Mass transit: epithelial morphogenesis in the *Drosophila* egg chamber. *Dev Dyn* 232, 559-574.
7. Tanentzapf, G., Smith, C., McGlade, J., and Tepass, U. (2000). Apical, lateral, and basal polarization cues contribute to the development of the follicular epithelium during *Drosophila* oogenesis. *J Cell Biol* 151, 891-904.
8. Niewiadomska, P., Godt, D., and Tepass, U. (1999). DE-Cadherin is required for intercellular motility during *Drosophila* oogenesis. *J Cell Biol* 144, 533-547.
9. Bai, J., Uehara, Y., and Montell, D.J. (2000). Regulation of invasive cell behavior by taiman, a *Drosophila* protein related to AIB1, a steroid receptor coactivator amplified in breast cancer. *Cell* 103, 1047-1058.
10. Yip, M.L., Lamka, M.L., and Lipshitz, H.D. (1997). Control of germ-band retraction in *Drosophila* by the zinc-finger protein HINDSIGHT. *Development* 124, 2129-2141.
11. Wilk, R., Reed, B.H., Tepass, U., and Lipshitz, H.D. (2000). The hindsight gene is required for epithelial maintenance and differentiation of the tracheal system in *Drosophila*. *Dev Biol* 219, 183-196.
12. Reed, B.H., Wilk, R., and Lipshitz, H.D. (2001). Downregulation of Jun kinase signaling in the amnioserosa is essential for dorsal closure of the *Drosophila* embryo. *Curr Biol* 11, 1098-1108.
13. Ito, K., Awano, W., Suzuki, K., Hiromi, Y., and Yamamoto, D. (1997). The *Drosophila* mushroom body is a quadruple structure of clonal units each of which contains a virtually identical set of neurones and glial cells. *Development* 124, 761-771.
14. Mathieu, J., Sung, H.H., Pugieux, C., Soetaert, J., and Rorth, P. (2007). A sensitized PiggyBac-based screen for regulators of border cell migration in *Drosophila*. *Genetics* 176, 1579-1590.
15. Silver, D.L., and Montell, D.J. (2001). Paracrine signaling through the JAK/STAT pathway activates invasive behavior of ovarian epithelial cells in *Drosophila*. *Cell* 107, 831-841.
16. Silver, D.L., Geisbrecht, E.R., and Montell, D.J. (2005). Requirement for JAK/STAT signaling throughout border cell migration in *Drosophila*. *Development* 132, 3483-3492.

17. Montell, D.J., Rorth, P., and Spradling, A.C. (1992). slow border cells, a locus required for a developmentally regulated cell migration during oogenesis, encodes Drosophila C/EBP. *Cell* 71, 51-62.
18. Ray, S.K., Nishitani, J., Petry, M.W., Fessing, M.Y., and Leiter, A.B. (2003). Novel transcriptional potentiation of BETA2/NeuroD on the secretin gene promoter by the DNA-binding protein Finb/RREB-1. *Mol Cell Biol* 23, 259-271.
19. Liang, C.C., Park, A.Y., and Guan, J.L. (2007). In vitro scratch assay: a convenient and inexpensive method for analysis of cell migration in vitro. *Nat Protoc* 2, 329-333.
20. Lie, Y.S., and Macdonald, P.M. (1999). Apontic binds the translational repressor Bruno and is implicated in regulation of oskar mRNA translation. *Development* 126, 1129-1138.

## Figure Legends

### **Figure 1. *hnt* regulates the levels of several adhesion proteins and is required for stretched follicle cell flattening**

(A-D) Micrographs of wild-type egg chambers of stage 8 (A and A'), early stage 9 (B and B'), mid stage 9 (C and C') and stage 10 (D and D') stained with ARM (green), DE-CAD (red) and DAPI (blue). Panels A-D show a focal plane near the center of the egg chamber whereas A'-D' show a superficial focal plane. Border cells (BC, arrowheads) form a cluster together with the non-motile polar cells (PC), and migrate in between the nurse cells (nc) towards the oocyte (o). Anterior "stretched" follicle cells (StFC) elongate along the anterior/posterior axis, and the rest of the follicle cells, so-called main body cells (MBFC) stack up over the oocyte. Insets in panels (A'-D') show anterior follicle cells (FC) labeled with membrane GFP (green) and DAPI. The expansion of the apical membrane, the flattening of the stretched follicle cells and the decrease in cell density can be appreciated. (E-K) Micrographs of egg chambers containing homozygous *hnt* mutant clones are GFP negative. *hnt* mutant stretched follicle cells accumulate ARM (E-E') and DN-CAD (F-F') in the plasma membrane and fail to flatten. *hnt* mutant main body follicle cells accumulate ARM (G-G'), DE-CAD (H-H'), DN-CAD (I-I'), and FASIII (J-J) but not F-actin (K-K') in the plasma membrane. The scale bar represents 50  $\mu\text{m}$  in A and E and 20  $\mu\text{m}$  in B-D' insets.

## Figure 2. *hnt* is required for collective migration of the border cells

(A) Wild type stage 10 egg chamber stained with HNT, DE-CAD and DAPI. HNT is highly expressed in the border cells and the stretched follicle cells. The border cell cluster has reached the oocyte (arrow). (B) *hnt* mutant border cells fail to initiate migration and stay at the anterior tip of the egg chamber (arrow). (C-D) high magnification of border cell clusters of stage 9 egg chambers (inset) stained with ARM (C, E) and GFP (C', E'). Wild type border cells (BC) and polar cells (PC) are GFP positive, *hnt* mutant border cells (BC\*) are GFP negative. (D-E) line scan across the center of the border cell clusters shown in C and E to show the levels of ARM at the indicated cell-cell contacts.

## Figure 3. High levels of *hnt* or low levels of JNK activity disrupt border cell cluster cohesiveness

(A-D) Micrographs of egg chambers of the indicated genotypes in which border cells are labeled with membrane-anchored GFP. (A) Wild type stage 10 egg chamber in which the border cell cluster (arrowhead) has reached the oocyte. (B) High magnification of a wild-type border cell cluster. (C and D) Over-expression of *hnt* using *slbo*-Gal4 driver and *hnt*<sup>EP55</sup> EP insertion. Border cells (arrowhead) fail to migrate and lose cohesiveness among each other. The scale bar in A represents 50  $\mu$ m and applies to A and C. The scale bar in B represents 20  $\mu$ m and applies to B and D. (E-F) Egg chambers stained with anti phospho-JUN (p-jun) and anti-apoptotic (APT) antibodies. (E) Control egg chamber showing expression pattern of p-jun in all the cells, including the migrating border cells (brackets). (F) An egg chamber in which *hnt* was over-expressed

in the border cells shows decreased p-jun staining. APT is a nuclear protein expressed in all the follicle cells including the border cells [20]. Unchanged nuclear localization of APT in the border cells was used as an internal control. (G-H) Egg chambers of the indicated genotypes stained with anti-SLBO and anti-GFP antibodies. *Puc2A* over-expressing border cells fail to complete migration and the cluster disassembles. The insets in (G-H) show the expression levels of *hnt* in egg chambers of the same genotypes as the main panels. The ratio of HNT to DAPI staining intensity is indicated. (I) The migration index (complete migration = 100; no migration = 0), and the border cell cluster radius are reported for each of the indicated genotypes. The standard error (SE) is indicated.

**Figure 4. Knockdown of RREB1 impairs migration in a mammary epithelial cells**

(A) Domain structure of RREB-1 and HNT with the C2H2 Zn finger domains indicated. (B) Knockdown of RREB1 in MCF-10A cells resulted in significantly impaired migration for the *SMART*pool relative to the mock-transfection control. Three of the four *SMART*pool constituent siRNAs (numbered 1-4) induced a consistent reduction in cell migration, thereby validating the *SMART*pool phenotype. (C) Knockdown of RREB1 for 48 hours and subsequent re-plating shows a marked reduction in cell spreading after plating at a similar density to control. Images are shown for different time points using different magnification (10X, 20X objectives).